

Spin relaxation in an InAs quantum dot in the presence of terahertz driving fields

J. H. Jiang and M. W. Wu*

*Hefei National Laboratory for Physical Sciences at Microscale,
University of Science and Technology of China, Hefei, Anhui, 230026, China and*

*Department of Physics, University of Science and Technology of China, Hefei, Anhui, 230026, China[†]
(Dated: March 23, 2022)*

The spin relaxation in a 1D InAs quantum dot with the Rashba spin-orbit coupling under driving THz magnetic fields is investigated by developing a kinetic equation with the help of the Floquet-Markov theory, which is generalized to the system with the spin-orbit coupling, to include both the strong driving field and the electron-phonon scattering. The spin relaxation time can be effectively prolonged or shortened by the terahertz magnetic field depending on the frequency and strength of the terahertz magnetic field. The effect can be understood as the sideband-modulated spin-phonon interaction. This offers an additional way to manipulate the spin relaxation time.

PACS numbers: 71.70.Ej, 72.25.Rb, 78.90.+t, 78.67.De

I. INTRODUCTION

One of the goals of semiconductor spintronics^{1,2} is to realize quantum information processing based on electron/hole spins. Coherent oscillations of spin state driven by an AC magnetic/electric field, which is the key of such a goal, have been broadly studied.^{3,4,5,6,7,8,9,10,11} Experiments have demonstrated successfully the coherent oscillations of electron spin by optical Stark effect in quantum wells on femtosecond time scale and by gigahertz-gate-voltage-controlled g -tensor modulation.^{3,9} Recently, driven coherent oscillations of single spin in quantum dots (QDs) at hundreds of MHz has also been realized.¹¹ Theoretically, Rashba and Efros showed perturbatively that electron spin can be manipulated by a weak in-plane time-dependent electric field via the spin-orbit coupling (SOC), such as the Rashba¹² and the Dresselhaus¹³ couplings.⁴ They called it the electric-dipole spin resonance (EDSR). Similar schemes have also been proposed in QDs.^{7,8} Cheng and Wu have discussed *non-perturbatively* the effect of an intense terahertz (THz) electric field on two-dimensional electron gas (2DEG) with the Rashba SOC where the spin splitting is of the order of THz.⁵ They showed that a THz electric field can strongly affect the density of states of the electron system and induce a THz spin oscillations. Similar effects have also been studied in QD by Jiang *et al.*⁶ However, up till now there is no study on the spin dissipation effect, *i.e.*, spin dephasing/relaxation in the AC-field driven systems, especially from a fully microscopic approach. Recently Duckheim and Loss have studied the EDSR in the presence of disorder in a 2DEG, where the dissipation effect is introduced by a relaxation time.¹⁰ It has been shown in the system without the SOC that the dissipation under driving field can be very different from the one without the driving field.^{14,15} A full microscopic kinetic equation under driving field can be developed with the help of Floquet-Markov theory.¹⁶ The Floquet-Markov theory combines the Floquet theory which can

solve the time-dependent (periodic) Schrödinger equation *non-perturbatively* with the Born-Markov approximation which is frequently used in deriving the kinetic equation with dissipations.

In the present paper, we extend the Floquet-Markov approach to the system with the SOC. The change in density of states by the THz laser field^{5,6} implies a modification of the spin related scattering and then the spin relaxation time. We study the spin relaxation in an InAs QD by developing a Floquet-Markov type kinetic equation with the electron-acoustic-phonon scattering. The spin relaxation time is obtained by numerically solving the kinetic equation. We develop the model and formalism in Sec. II and present the numerical results in Sec. III. We conclude in Sec. IV.

II. MODEL AND FORMALISM

We construct our theory in a 1D QD in which electron is strongly confined in the x - y directions and relatively weaker along the z -axis. This kind of QDs have been realized experimentally and are attracting more and more interests due to the good controllability of the size, shape, position, and electronic structures.^{17,18} A static magnetic field and a THz electric/magnetic field, which can be provided by the free electron laser,¹⁹ are applied along the z -axis. The total Hamiltonian is then given by

$$H_{tot} = H_e + H_p + H_{ep}, \quad (1)$$

with $H_p = \sum_{\mathbf{q}\eta} \hbar\omega_{\mathbf{q}\eta} a_{\mathbf{q}\eta}^\dagger a_{\mathbf{q}\eta}$ and $H_{ep} = \sum_{\mathbf{q}\eta} M_{\mathbf{q}\eta} (a_{\mathbf{q}\eta} + a_{-\mathbf{q}\eta}^\dagger) \exp(i\mathbf{q} \cdot \mathbf{r})$ representing the phonon and the electron-phonon interaction Hamiltonian respectively. The electron Hamiltonian in the Coulomb gauge reads²⁰

$$H_e = \frac{\mathbf{P}^2}{2m^*} + V_c(\mathbf{r}) + H_{so}(\mathbf{P}) + H_Z, \quad (2)$$

in which $\mathbf{P} = -i\hbar\nabla + e/c\mathbf{A}(t)$ with $\mathbf{A}(t) = -c\mathbf{E}_1 \cos(\Omega t)/\Omega + \frac{1}{2}[\mathbf{B}_0 + \mathbf{B}_1 \cos(\Omega t)] \times \mathbf{r}$ denoting the

vector potential induced by the THz electric/magnetic field and the static magnetic field. m^* denotes the electron effective mass. $V_c(\mathbf{r})$ is the confining potential of the QD which is taken to be square well with infinite well depth in each direction.¹⁸ $H_{so}(\mathbf{P})$ is the SOC term, which consists of the Rashba term due to the structure inversion asymmetry¹² and the Dresselhaus term due to the bulk inversion asymmetry.¹³ In InAs the Rashba SOC is the dominant contribution. $H_Z = \frac{1}{2}g\mu_B(\mathbf{B}_0 + \mathbf{B}_1 \cos(\Omega t)) \cdot \boldsymbol{\sigma}$ represents the Zeeman term. When the transverse confinement is strong enough, only the lowest subband is considered. Then the Hamiltonian of the electron can be reduced to an effective Hamiltonian $H_{eff} = \frac{P_z^2}{2m^*} + V(z) + H_{so}^R(P_z) + H_Z$, where $P_z = p_z - eE_1 \cos(\Omega t)/\Omega$ and $p_z = -i\hbar \frac{\partial}{\partial z}$. The Rashba term is $H_{so}^R = \frac{e\gamma_R}{\hbar}(\sigma_x E_y - \sigma_y E_x)P_z$ with E_x and E_y being the electric fields along the x - and y -directions which are due to the structure inversion asymmetry and can be controlled by the gate voltage.²¹ For simplicity we choose $E_y = 0$ in our investigation and $H_{so}^R = -e\frac{\gamma_R}{\hbar}E_x\sigma_y P_z \equiv \frac{\alpha_R}{\hbar}\sigma_y P_z$. This choice will not change the results of the calculation as one can always take a unitary transformation in the spin space to transfer any other configuration into our simplified one. The effective Hamiltonian is then written as

$$H_{eff}(t) = H_0 + H_1(t) + H_2(t), \quad (3)$$

with

$$H_0 = \frac{p_z^2}{2m^*} + V(z) + \frac{\alpha_R}{\hbar}\sigma_y p_z + \frac{1}{2}g\mu_B B_0 \sigma_z, \quad (4)$$

$$H_1(t) = [\frac{1}{2}g\mu_B B_1 \sigma_z - \frac{eE_1}{\Omega}(\frac{p_z}{m^*} + \frac{\alpha_R}{\hbar}\sigma_y)] \cos(\Omega t), \quad (5)$$

$$H_2(t) = \frac{e^2 E_1^2 \cos^2(\Omega t)}{2m^* \Omega^2}. \quad (6)$$

Hence $H_{eff}(t+T_{ac}) = H_{eff}(t)$ and $T_{ac} = \frac{2\pi}{\Omega}$. We observe that $H_2(t)$ is only a function of time, and does not contain any other physical variables of electron. Thus it only induces a universal phase and has no contribution to the kinetics of the system. The corresponding Schrödinger equation

$$i\hbar \frac{\partial}{\partial t} \Psi(t) = H_{eff}(t) \Psi(t) \quad (7)$$

can be solved via the Floquet-Fourier approach developed by Shirley²² and applied lately in systems with the SOC by Cheng and Wu.⁵ The solution is

$$\Psi_\lambda(z, t) = e^{-i\varepsilon_\lambda t} \sum_{n=-\infty}^{\infty} \sum_{\alpha} F_{n\alpha}^\lambda \phi_\alpha(z) e^{in\Omega t}, \quad (8)$$

in which $\{\phi_\alpha(z)\}$ is a complete set of the wave functions, chosen here to be the eigen-functions of a infinite-depth-square-well potential $V(z)$.^{5,6} $\{\varepsilon_\lambda\}$ and $\{F_{n\alpha}^\lambda\}$ are the quasi-energies and the eigen-vectors of the following

equations:²²

$$\sum_{m=-\infty}^{\infty} \sum_{\beta} \langle \alpha n | \mathcal{H}_F | \beta m \rangle F_{m\beta}^\lambda = \varepsilon_\lambda F_{n\alpha}^\lambda, \quad (9)$$

where $\langle \mathbf{r}, t | \alpha n \rangle \equiv \phi_\alpha(\mathbf{r}) e^{in\Omega t}$, $\mathcal{H}_F = H_{eff}(t) - i\partial_t$ and $\langle \alpha n | \mathcal{H}_F | \beta m \rangle = H_{\alpha\beta}^{n-m} + m\Omega \delta_{\alpha\beta} \delta_{nm}$ with $H^n = \frac{1}{T} \int_0^T dt e^{-in\Omega t} H_{eff}(t)$ representing the n -th Fourier component of the effective Hamiltonian. Due to the periodicity of \mathcal{H}_F , the eigenvalues are also periodic and can be written as $\varepsilon_{\lambda,l} = \varepsilon_{\lambda,0} + l\Omega$ where $\varepsilon_{\lambda,0}$ is the eigenvalue in the region $(-\Omega/2, \Omega/2]$. It is noted that $\varepsilon_{\lambda,l}$ and $\varepsilon_{\lambda,0}$ correspond to the same physical solution to the Schrödinger equation. In the following we denote $\varepsilon_{\lambda,0}$ with ε_λ for simplicity. The eigenvectors of the eigen-equations satisfy the orthogonal and complete relations

$$\sum_{n,\alpha} F_{n\alpha}^{\lambda_1, l_1*} F_{n\alpha}^{\lambda_2, l_2} = \delta_{\lambda_1 \lambda_2} \delta_{l_1 l_2}, \quad (10)$$

$$\sum_{\lambda, l} F_{n_1 \alpha_1}^{\lambda, l*} F_{n_2 \alpha_2}^{\lambda, l} = \delta_{\alpha_1 \alpha_2} \delta_{n_1 n_2}. \quad (11)$$

From these relations one obtains the orthogonal and complete relations of the Floquet wavefunctions^{14,22}

$$\sum_{\lambda} \Psi_\lambda^*(z, t) \Psi_\lambda(z', t) = \delta(z - z'), \quad (12)$$

$$\int_{-\infty}^{\infty} dz \Psi_\lambda^*(z, t) \Psi_{\lambda'}(z, t) = \delta_{\lambda, \lambda'}. \quad (13)$$

The wavefunction [Eq. (8)] includes two significant effects, one is the sideband effect²³ and the other is the AC Stark effect.²⁴ The former refers to the many frequencies $\varepsilon_\lambda - n\Omega$ in the wavefunction and the later represents the field-induced change of ε_λ .

The Floquet wavefunctions which contain all the dynamic properties of the electron system without the electron-phonon coupling, give an optimal base to solve the equation of motion of the reduced density matrix of the electron system. The Floquet-Markov method which combines the Floquet solution of the electron Hamiltonian and the Born-Markov approach to solve the equation of motion under strong AC driving field was developed by Kohler *et al.* in the absence of the SOC.¹⁶ Generally this method works well when the AC driven electron system is in the dynamic stable regime and the system interacts weakly with a Markovian reservoir with a damping rate much less than any eigen-frequency of the system. The latter requirement can be satisfied for almost every case in the spin decoherence problem, as spins are generally expected to have a very long coherence time.²⁵ In addition, studies have shown that, as well as keeping good quantitative results, the Floquet-Markov method has the advantage of being easy to handle numerically compared with the rather complicated path-integral approach.¹⁶ Thus this method is very useful in the study of relaxation/dephasing in nano-structures. In

the present paper, we apply this method to the systems with the SOC to study the spin relaxation in QD due to the electron-acoustic-phonon scattering under the THz driving field.

With the standard Feynman-Vernon initial condition $\rho(t_0) = \rho^e(t_0) \otimes \rho_{eq}^p$, where ρ is the density matrix of the

electron and phonon system; ρ^e is the density matrix of the electron system and ρ_{eq}^p represents the density matrix of the equilibrium phonon reservoir, and within the Born-Markov approximation, the reduced density matrix of the electron system satisfies the following equation:

$$\frac{\partial}{\partial t} \rho^e = -\frac{i}{\hbar} [H_e(t), \rho^e] - \frac{1}{\hbar^2} \int_0^\infty d\tau \text{Tr}_p \{ [H_{ep}, [\tilde{H}_{ep}(t-\tau, t), \rho^e \otimes \rho_{eq}^p]] \} \quad (14)$$

with Tr_p standing for the trace over the phonon degree of freedom. $\tilde{H}_{ep}(t-\tau, t) = U_0^\dagger(t-\tau, t) H_{ep} U_0(t-\tau, t)$, in which $U_0(t-\tau, t) = \mathcal{P}_t \exp[-\frac{i}{\hbar} \int_t^{t-\tau} dt' (H_e(t') + H_p)]$ with \mathcal{P}_t denoting the time-ordering operator. Next we express this integral-differential equation of operators in a complete base of Floquet wavefunctions denoted by $\{|\lambda(t)\rangle\}$. Using the complete relation $\sum_\lambda |\lambda(t)\rangle \langle \lambda(t)| = 1$,^{14,22} after some simple algebra, one has

$$\begin{aligned} \frac{\partial}{\partial t} \rho_{\lambda_1 \lambda_2}^e &= -\frac{1}{\hbar^2} \int_0^\infty d\tau \sum_{\lambda_3 \lambda_4} \text{Tr}_p (H_{\lambda_1 \lambda_3}^{ep} \tilde{H}_{\lambda_3 \lambda_4}^{ep} \rho_{\lambda_4 \lambda_2}^e \otimes \rho_{eq}^p - \tilde{H}_{\lambda_1 \lambda_3}^{ep} \rho_{\lambda_3 \lambda_4}^e \otimes \rho_{eq}^p H_{\lambda_4 \lambda_2}^{ep}) + H.c. \\ &= -\frac{1}{\hbar^2} \int_0^\infty d\tau \sum_{\lambda_3 \lambda_4} \sum_{\mathbf{q}\eta} (X_{\lambda_1 \lambda_3}^{\mathbf{q}} \tilde{X}_{\lambda_3 \lambda_4}^{-\mathbf{q}} \rho_{\lambda_4 \lambda_2}^e - \tilde{X}_{\lambda_1 \lambda_3}^{-\mathbf{q}} \rho_{\lambda_3 \lambda_4}^e X_{\lambda_4 \lambda_2}^{\mathbf{q}}) \langle \langle A_{\mathbf{q}\eta}(\tau) A_{-\mathbf{q}\eta} \rangle \rangle + H.c. \end{aligned} \quad (15)$$

where $X_{\lambda_1 \lambda_2}^{\mathbf{q}} = \langle \lambda_1(t) | \exp(i\mathbf{q} \cdot \mathbf{r}) | \lambda_2(t) \rangle$, $A_{\mathbf{q}\eta}(t) = M_{\mathbf{q}\eta} (a_{-\mathbf{q}\eta}^\dagger e^{i\omega_{\mathbf{q}\eta} t} + a_{\mathbf{q}\eta} e^{-i\omega_{\mathbf{q}\eta} t})$ and $\tilde{X}_{\lambda_1 \lambda_2}^{\mathbf{q}} = \langle \lambda_1(t) | U_0^\dagger(t-\tau, t) \exp(i\mathbf{q} \cdot \mathbf{r}) U_0(t-\tau, t) | \lambda_2(t) \rangle$ with $U_0(t-\tau, t) = \mathcal{P}_t \exp[-\frac{i}{\hbar} \int_t^{t-\tau} dt' H_e(t')]$. $\langle \langle \cdots \rangle \rangle$ in Eq. (15) represents the statistical average over the phonon equilibrium distribution. By substituting the Floquet wave functions into X , one obtains $X_{\lambda_1 \lambda_2}^{\mathbf{q}} = \sum_k e^{i\Delta_{\lambda_1 \lambda_2 k} t} X_{\lambda_1 \lambda_2 k}^{\mathbf{q}}$ where $\Delta_{\lambda_1 \lambda_2 k} = (\varepsilon_{\lambda_1} - \varepsilon_{\lambda_2})/\hbar + k\Omega$ and $X_{\lambda_1 \lambda_2 k}^{\mathbf{q}} = \sum_n \sum_\alpha \sum_\beta F_{n\alpha}^{\lambda_1 *} F_{n+k\beta}^{\lambda_2} \langle \alpha | \exp(i\mathbf{q} \cdot \mathbf{r}) | \beta \rangle = X_{\lambda_2 \lambda_1 -k}^{\mathbf{q}*}$. As the Floquet wavefunctions are the solutions to Eq. (7), one has

$$\begin{aligned} \tilde{X}_{\lambda_1 \lambda_2}^{\mathbf{q}} &= \langle \lambda_1(t) | U_0^\dagger(t-\tau, t) \exp(i\mathbf{q} \cdot \mathbf{r}) U_0(t-\tau, t) | \lambda_2(t) \rangle = \langle \lambda_1(t-\tau) | \exp(i\mathbf{q} \cdot \mathbf{r}) | \lambda_2(t-\tau) \rangle \\ &= \sum_k e^{i\Delta_{\lambda_1 \lambda_2 k} (t-\tau)} X_{\lambda_1 \lambda_2 k}^{\mathbf{q}}. \end{aligned} \quad (16)$$

Therefore, Eq. (15) reads

$$\begin{aligned} \frac{\partial}{\partial t} \rho_{\lambda_1 \lambda_2}^e &= -\frac{1}{\hbar^2} \sum_{\lambda_3 \lambda_4} \sum_{k_1 k_2} \sum_{\mathbf{q}\eta} \pi |M_{\mathbf{q}\eta}|^2 \{ X_{\lambda_1 \lambda_3 k_1}^{\mathbf{q}} X_{\lambda_4 \lambda_3 k_2}^{\mathbf{q}*} \rho_{\lambda_4 \lambda_2}^e e^{i(\Delta_{\lambda_1 \lambda_3 k_1} - \Delta_{\lambda_4 \lambda_3 k_2}) t} C_{\mathbf{q}\eta}(\Delta_{\lambda_4 \lambda_3 k_2}) \\ &\quad - X_{\lambda_4 \lambda_2 k_1}^{\mathbf{q}} X_{\lambda_3 \lambda_1 k_2}^{\mathbf{q}*} \rho_{\lambda_3 \lambda_4}^e e^{i(\Delta_{\lambda_4 \lambda_2 k_1} - \Delta_{\lambda_3 \lambda_1 k_2}) t} C_{\mathbf{q}\eta}(\Delta_{\lambda_3 \lambda_1 k_2}) \} + H.c., \end{aligned} \quad (17)$$

with $C_{\mathbf{q}\eta}(\Delta) = \bar{n}(\omega_{\mathbf{q}\eta}) \delta(\Delta + \omega_{\mathbf{q}\eta}) + (\bar{n}(\omega_{\mathbf{q}\eta}) + 1) \delta(\Delta - \omega_{\mathbf{q}\eta})$. Here $\bar{n}(\omega_{\mathbf{q}\eta})$ is the Bose distribution function. The summations over k_1 and k_2 range from $-\infty$ to ∞ . The terms with $C_{\mathbf{q}\eta}(\Delta_{\lambda_3 \lambda_1 k_2})$ describe the k_2 -photon-assisted scattering. These equations are still time-dependent. With the rotating wave approximation (RWA), one can sweep out the time-dependent terms which oscillate much faster than the damping rate of the density matrix¹⁶ and Eq. (17) is further simplified into

$$\frac{\partial}{\partial t} \rho_{\lambda_1 \lambda_2}^e = - \sum_{\lambda_3 \lambda_4} \Lambda_{\lambda_1 \lambda_2 \lambda_3 \lambda_4} \rho_{\lambda_3 \lambda_4}^e \quad (18)$$

with

$$\begin{aligned} \Lambda_{\lambda_1 \lambda_2 \lambda_3 \lambda_4} &= \left\{ \frac{1}{\hbar^2} \sum_{k_1, k_2} \sum_{\mathbf{q}\eta} \pi |M_{\mathbf{q}\eta}|^2 \left[\sum_{\lambda_5} X_{\lambda_1 \lambda_5 k_1}^{\mathbf{q}} X_{\lambda_1 \lambda_5 k_2}^{\mathbf{q}*} \delta_{k_1, k_2} \delta_{\lambda_1, \lambda_3} \delta_{\lambda_2, \lambda_4} C_{\mathbf{q}\eta}(\Delta_{\lambda_1 \lambda_5 k_2}) \right. \right. \\ &\quad \left. \left. - X_{\lambda_4 \lambda_2 k_1}^{\mathbf{q}} X_{\lambda_3 \lambda_1 k_2}^{\mathbf{q}*} \delta_{\varepsilon_{\lambda_4} - \varepsilon_{\lambda_2} - \varepsilon_{\lambda_3} + \varepsilon_{\lambda_1}, (k_2 - k_1)\Omega} C_{\mathbf{q}\eta}(\Delta_{\lambda_3 \lambda_1 k_2}) \right] \right\} + \left\{ \lambda_1 \leftrightarrow \lambda_2, \lambda_3 \leftrightarrow \lambda_4 \right\}^* \end{aligned} \quad (19)$$

being a time-independent tensor in the case without de-

generacy. $\{\lambda_1 \leftrightarrow \lambda_2, \lambda_3 \leftrightarrow \lambda_4\}^*$ in the above equation

stands for the same terms as in the previous $\{\}$ but interchanging λ_1 and λ_2 , λ_3 and λ_4 and taking a complex conjugate. In the zero driving field limit, the Floquet wavefunction reduces from a many-frequency one to a single-frequency one. Thus, the only nonzero contribution in the summation $X_{\lambda_1\lambda_2}^{\mathbf{q}} = \sum_k e^{i\Delta_{\lambda_1\lambda_2k}t} X_{\lambda_1\lambda_2k}^{\mathbf{q}}$ is the term with $k = k_0$, with $\hbar\Delta_{\lambda_1\lambda_2k_0} = E_{\lambda_1} - E_{\lambda_2}$ being the energy difference between states $|\lambda_1\rangle$ and $|\lambda_2\rangle$. $\delta_{\varepsilon_{\lambda_4} - \varepsilon_{\lambda_2} - \varepsilon_{\lambda_3} + \varepsilon_{\lambda_1}, (k_2 - k_1)\Omega}$ can be simplified into $(\delta_{\lambda_1, \lambda_3} \delta_{\lambda_2, \lambda_4} + \delta_{\lambda_1, \lambda_2} \delta_{\lambda_3, \lambda_4})$. Therefore Eq. (18) can be simplified into

$$\begin{aligned} \frac{\partial}{\partial t} \rho_{\lambda_1\lambda_2}^e &= \left\{ -\frac{\pi}{\hbar^2} \sum_{\mathbf{q}\eta, \lambda_3} |M_{\mathbf{q}\eta}|^2 |\langle \lambda_1 | e^{i\mathbf{q}\cdot\mathbf{r}} | \lambda_3 \rangle|^2 \rho_{\lambda_1\lambda_2}^e \right. \\ &\quad \times [\bar{n}(\omega_{\mathbf{q}\eta}) \delta(E_{\lambda_1} - E_{\lambda_3} + \omega_{\mathbf{q}\eta}) \\ &\quad \left. + (\bar{n}(\omega_{\mathbf{q}\eta}) + 1) \delta(E_{\lambda_1} - E_{\lambda_3} - \omega_{\mathbf{q}\eta}) \right\} \\ &\quad + \left\{ \lambda_1 \leftrightarrow \lambda_2 \right\}^* \end{aligned} \quad (20)$$

for $\lambda_1 \neq \lambda_2$, where E_λ is the energy of the state $|\lambda\rangle$ and

$$\begin{aligned} \frac{\partial}{\partial t} \rho_{\lambda_1\lambda_1}^e &= -\frac{2\pi}{\hbar^2} \sum_{\mathbf{q}\eta} |M_{\mathbf{q}\eta}|^2 \left\{ \sum_{\lambda_3} |\langle \lambda_1 | e^{i\mathbf{q}\cdot\mathbf{r}} | \lambda_3 \rangle|^2 \rho_{\lambda_1\lambda_1}^e \right. \\ &\quad \times [\bar{n}(\omega_{\mathbf{q}\eta}) \delta(E_{\lambda_1} - E_{\lambda_3} + \omega_{\mathbf{q}\eta}) \\ &\quad \left. + (\bar{n}(\omega_{\mathbf{q}\eta}) + 1) \delta(E_{\lambda_1} - E_{\lambda_3} - \omega_{\mathbf{q}\eta}) \right] \\ &\quad - \sum_{\lambda_2} |\langle \lambda_1 | e^{i\mathbf{q}\cdot\mathbf{r}} | \lambda_2 \rangle|^2 \rho_{\lambda_2\lambda_2}^e [\bar{n}(\omega_{\mathbf{q}\eta}) \delta(E_{\lambda_2} - E_{\lambda_1} + \omega_{\mathbf{q}\eta}) \\ &\quad \left. + (\bar{n}(\omega_{\mathbf{q}\eta}) + 1) \delta(E_{\lambda_2} - E_{\lambda_1} - \omega_{\mathbf{q}\eta}) \right\}. \end{aligned} \quad (21)$$

These equations are consistent with the kinetic spin Bloch equations.²⁶

Equation (18) can be rewritten in the matrix form as $\frac{\partial}{\partial t} \rho^e = -\mathbf{\Lambda} \rho^e$, which is a standard first order differential equation. It can be solved through the eigenvalues and eigenvectors of the matrix $\mathbf{\Lambda}$. Thus, for any observable \hat{O} ,

$$\begin{aligned} O(t) &= \text{Tr}(\hat{O} \rho^e) \\ &= \sum_{\lambda_1 \dots \lambda_6} \langle \lambda_2(t) | \hat{O} | \lambda_1(t) \rangle \mathbf{P}_{(\lambda_1\lambda_2)(\lambda_3\lambda_4)} \\ &\quad \times e^{-\mathbf{\Gamma}_{(\lambda_3\lambda_4)} t} \mathbf{P}_{(\lambda_3\lambda_4)(\lambda_5\lambda_6)}^{-1} \rho_{\lambda_5\lambda_6}^e(0) \end{aligned} \quad (22)$$

with $\mathbf{\Gamma} = \mathbf{P}^{-1} \mathbf{\Lambda} \mathbf{P}$ being a diagonal matrix and \mathbf{P} being the transformation matrix. By solving Eqs. (8), (9), (19) and (22) numerically with an initial spin polarization $S_z(0)$, one obtains the time evolution of S_z .

III. NUMERICAL RESULTS

We consider an isolated 1D InAs QD, where the low-lying states can be approximated by eigenstates in an infinite-well-depth potential:¹⁸ $V_c(\mathbf{r}) = 0$ if $0 < x < L_a$, $0 < y < L_b$ and $0 < z < L_c$ and $V_c(\mathbf{r}) = \infty$ elsewhere.

We choose $L_a = L_b = 20$ nm and $L_c = 70$ nm in the calculation. The separation between the first and the second subbands is about 9 meV (15 THz) along the z -direction, and 120 meV along the x (or y)-direction. By averaging over the lowest states in the x and y directions, one can turn the problem into an effective 1D problem. We apply a static magnetic field B_0 of 0.5/0.7/1 T along the z -axis which corresponds to a Zeeman splitting of about 0.4/0.56/0.8 meV (0.62/0.87/1.25 THz). In this energy range the electron-acoustic-phonon scattering is dominated by the deformation potential coupling in InAs. The corresponding scattering matrix reads $M_{\mathbf{q}sl} = \Xi \sqrt{\hbar q / 2D} v_{sl}$, where Ξ is the deformation potential, D denotes the volume density and v_{sl} stands for the longitudinal sound velocity. All the parameters used in the calculation are listed in Table I.²⁷ We take the cut-off frequency of the phonon reservoir to be the Debye frequency ω_D . The temperature is taken to be 200 mK, corresponding to an energy of 0.016 meV (0.026 THz), which is quite smaller than the other energies of the system (especially the Zeeman splitting energy), *i.e.*, we study the spin relaxation in low temperature regime where the phonon-absorption processes are energetically unfavorable. The Rashba parameter is taken to be $\alpha_R = 3.0 \times 10^{-9}$ eV·cm.²¹ By including all the scattering processes between the Floquet states due to the electron-phonon scattering, one can calculate the scattering matrix $\mathbf{\Lambda}$ [Eq. (19)]. With a preparation of occupying the first excited Zeeman state of H_0 [see Eq.(4)] as the initial state, one can obtain the time-evolution of S_z . By taking the envelope of S_z and subtracting the equilibrium spin polarization, we define T_1 as the time needed for decay of the spin polarization by a factor of $1/e$.

D	$5.9 \times 10^3 \text{ kg/m}^3$	g	-14.7
v_{sl}	$4.28 \times 10^3 \text{ m/s}$	ω_D	32.7 THz
Ξ	5.8 eV	m^*	0.0239 m_0

TABLE I: Parameters used in the calculation

At the very low temperature we study, the spin relaxation is due to the spin-flip transition between the lowest Zeeman sublevels. Recently Fonseca-Romero *et al.* studied a model two-level system coupled to an Ohmic reservoir via σ_x .²⁸ They showed that the pseudo-spin relaxation and dephasing can be greatly modified by the driving field when it is in the type of $A\sigma_z \cos(\Omega t)$. Their results show that at low temperature when the frequency is below the cut-off frequency of the reservoir, the driving field enhances the pseudo-spin relaxation, otherwise impedes it. However, in QDs, spin is coupled indirectly with the phonon bath via the SOC. The effective spectral density of the spin-phonon coupling is generally not Ohmic.²⁹ Remarkably, in QD this spectral density can be controlled by the QD geometry (size, growth-direction, etc.), magnetic field, gate-voltage and the strength and symmetry of the SOC.^{29,30,31,32,33,34,35,36,37}

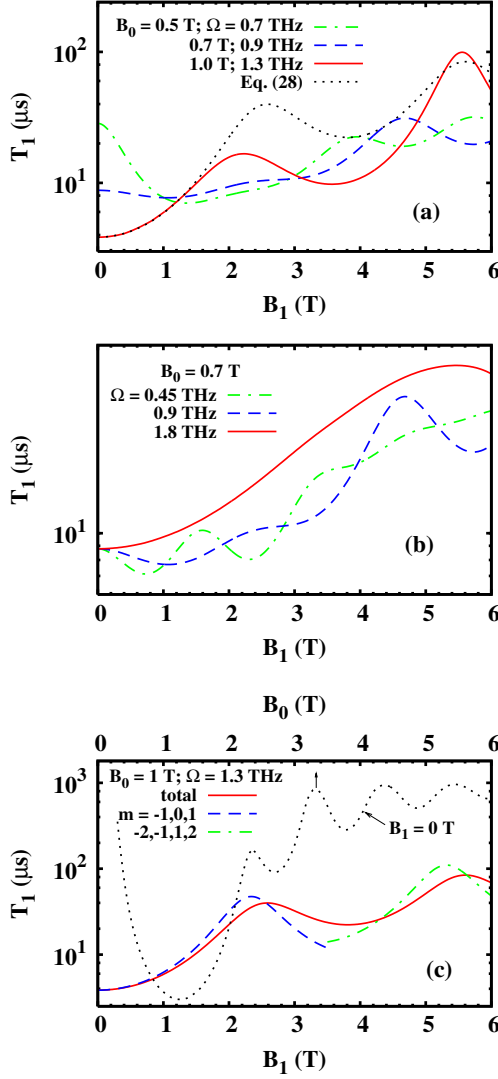


FIG. 1: (Color online) Spin relaxation time T_1 as a function of THz magnetic field strength B_1 for (a) $B_0 = 0.5$ T and $\Omega = 0.7$ THz (green chain curve); $B_0 = 0.7$ T and $\Omega = 0.9$ THz (blue dashed curve); $B_0 = 1.0$ T and $\Omega = 1.3$ THz (red solid curve), all in resonance, and (b) $B_0 = 0.7$ T, $\Omega = 0.45$ THz (green chain curve); 0.9 THz (blue dashed curve, in resonance); and 1.8 THz (red solid curve). The black dotted curve in (a) is the spin relaxation time calculated from the simplified model Eq. (28) for $B_0 = 1.0$ T and $\Omega = 1.3$ THz. (c) The spin relaxation time as a function of B_0 without the THz magnetic field (black dotted curve), and results from Eq. (28) including all sidebands (red solid curve); only the 0, and ± 1 -th sideband (blue dashed curve), and only the ± 1 and ± 2 -th sideband (green chain curve). Note the scale of B_0 is on the upper frame of the figure.

In our study, we investigate the spin relaxation in an InAs 1D QD in the presence of a THz driving magnetic field (no THz electric field included) along the z -axis (whose frequency is *below* the cut-off frequency) from a full microscopic approach. By including enough base-states and using the exact numerical diagonaliza-

tion method,³⁰ we can calculate the Floquet wavefunctions. We then substitute these wavefunctions into the kinetic equations Eq. (18) to obtain the dissipative dynamics of spin in QD under the driving field. We find that differing from the Ohmic spin-phonon coupling,²⁸ the spin relaxation time here can be either prolonged or shortened by the sideband effect, depending on the frequency and strength of both the THz magnetic field and the static magnetic field, with the latter providing the Zeeman splitting.

We plot the spin relaxation time T_1 as a function of the THz magnetic field B_1 in Fig. 1(a) with the electric field $E = 0$. The green-chain/blue-dashed/red-solid curves correspond to $B_0 = 0.5/0.7/1.0$ T and $\Omega = 0.7/0.9/1.3$ THz respectively. The THz magnetic field is tuned to be in resonance with the Zeeman splitting. It is seen from the figure that the spin relaxation time T_1 increases with the strength of the THz magnetic field B_1 , with some modulations. It increases more rapidly for the case with $B_0 = 1.0$ T than the other two cases: at $B_1 \approx 5.6$ T, T_1 is increased about 25 times of the value at $B_1 = 0$. It is also noted that due to the different modulations, when $B_1 \leq 1$ T, the spin relaxation time T_1 decreases rapidly/mildly for $B_0 = 0.5$ T/ 0.7 T but increases rapidly for $B_0 = 1.0$ T. We also plot T_1 at $E = 0$, and $B_0 = 0.7$ T as a function of B_1 with different frequencies (0.45, 0.9, and 1.8 THz) in Fig. 1(b). Again the spin relaxation time increases overall with B_1 but with different modulations. Nevertheless as a result of the modulation, when $B_1 \leq 0.7$ T, T_1 decreases for the case with $\Omega = 0.45$ THz and 0.9 THz (mildly) but increases for the case with $\Omega = 1.8$ THz.

These numerical results can be understood from the following simplified analysis. At zero electric field $E = 0$, the effective Hamiltonian [Eqs. (3-6)] in the matrix element form reads

$$\langle n, \sigma | H_{eff} | n', \sigma' \rangle = \left\{ E_n^0 + \frac{1}{2} [E_z^0 + E_z^1 \cos(\Omega t)] \sigma \right\} \delta_{n,n'} \times \delta_{\sigma,\sigma'} + E^{so}(n, \sigma; n', \sigma') \delta_{(-1)^n n' + 1 = 0} \delta_{\sigma+\sigma'=0}, \quad (23)$$

with $\langle z | n \rangle = \sqrt{\frac{2}{L_c}} \sin(\frac{n\pi z}{L_c})$, and $|\sigma\rangle$, the eigen vector of σ_z . $E_n^0 = n^2 \hbar^2 \pi^2 / (2m^* L_c^2)$ is the subband energy. $E_z^0 = g\mu_B B_0$ and $E_z^1 = g\mu_B B_1$ represent the spin splittings due to the static and the THz magnetic field. $E^{so}(n, \sigma; n', -\sigma) = \sigma \alpha_R \langle n | \frac{i}{\hbar} p_z | n' \rangle = \sigma \frac{4\alpha_R n n'}{L_c(n'^2 - n^2)}$. The last term of Eq. (23), which is the energy due to the SOC, is nonzero only for states with different spin and different parity. For very low temperature and for not too strong THz magnetic field, we can restrict ourselves to consider only the lowest two states due to the Zeeman splitting described by the time-independent parts of the effective Hamiltonian Eq. (23). These two states, denoted as $|\xi_\sigma\rangle$ with $\sigma = \uparrow, \downarrow$ (+, -), read

$$|\xi_\sigma\rangle \approx |1, \sigma\rangle + \sum_n \frac{E^{so}(2n, -\sigma; 1, \sigma)}{E_1 - E_{2n} + E_z \sigma} |2n, -\sigma\rangle, \quad (24)$$

from the perturbation. The matrix elements of the effective Hamiltonian in the space of these two states are $\langle \xi_\sigma | H_{eff} | \xi_{\sigma'} \rangle \approx \frac{1}{2} [E_z + g\mu_B B_1 \cos(\Omega t)] \sigma \delta_{\sigma, \sigma'}$ approximately by retaining only the dominant terms. E_z is the energy difference of the lowest two levels of H_0 which is approximately $g\mu_B B_0$ for not too large B_0 . For this Hamiltonian the Schödinger equation can be integrated out directly. The Floquet wavefunctions are therefore

$$\begin{aligned} \Psi_\sigma(t) &= \exp\left\{-i\left[\frac{\sigma g\mu_B B_0 t}{2\hbar} + \frac{\sigma g\mu_B B_1}{2\hbar\Omega} \sin(\Omega t)\right]\right\} \xi_\sigma \\ &= \exp\left(-i\frac{\sigma g\mu_B B_0 t}{2\hbar}\right) \sum_m J_m\left(\frac{\sigma g\mu_B B_1}{2\hbar\Omega}\right) \\ &\quad \times \exp(-im\Omega t) \xi_\sigma, \end{aligned} \quad (25)$$

in which J_m is the m -th Bessel function of the first kind and ξ_σ represents the pseudo-spin wavefunction of the lowest two states [Eq. (24)]. The form of the wavefunction clearly indicates the sideband effect. Specifically, the probability of finding the electron in $|\Psi_\sigma\rangle$ is $|J_m(\frac{\sigma g\mu_B B_1}{2\hbar\Omega})|^2$ which oscillates at a frequency $\sigma g\mu_B B_0/\hbar + m\Omega$. The frequency together with its corresponding coefficient $J_m(\frac{\sigma g\mu_B B_1}{2\hbar\Omega})$ is referred to as the m -th sideband from now on. In the following we show that this sideband effect can greatly affect the spin relaxation.

Substituting these wavefunctions into the kinetic equation Eq. (17), one obtains the following scattering matrix

$$\begin{aligned} \Lambda_{\uparrow\uparrow\uparrow\uparrow} &= \frac{2\pi}{\hbar^2} \sum_{\mathbf{q}\eta} |M_{\mathbf{q}\eta}|^2 \sum_k |X_{\uparrow\downarrow k}^{\mathbf{q}}|^2 C_{\mathbf{q}\eta}(\Delta_{\uparrow\downarrow k}) \\ &= \sum_k \Gamma(\Delta_{\uparrow\downarrow k}) \sum_{m, m'} J_{-m} J_{m+k} J_{-m'} J_{m'+k} \left(\frac{g\mu_B B_1}{2\hbar\Omega}\right) \\ &= \sum_k \Gamma(\Delta_{\uparrow\downarrow k}) J_k^2\left(\frac{g\mu_B B_1}{\hbar\Omega}\right). \end{aligned} \quad (26)$$

Here the relation $\sum_m J_{-m} J_{m+k}(x) = J_k(2x)$ is applied and

$$\begin{aligned} \Gamma(\Delta_{\uparrow\downarrow k}) &= \frac{2\pi}{\hbar^2} \sum_{\mathbf{q}\eta} |M_{\mathbf{q}\eta}|^2 |\langle \xi_\uparrow | e^{i\mathbf{q}\cdot\mathbf{r}} | \xi_\downarrow \rangle|^2 [\bar{n}(\omega_{\mathbf{q}\eta}) \\ &\quad \times \delta(\Delta_{\uparrow\downarrow k} + \omega_{\mathbf{q}\eta}) + (\bar{n}(\omega_{\mathbf{q}\eta}) + 1) \delta(\Delta_{\uparrow\downarrow k} - \omega_{\mathbf{q}\eta})]. \end{aligned} \quad (27)$$

Without the driving field, Eq. (26) reduces back to the well known form $\Lambda_{\uparrow\uparrow\uparrow\uparrow} = \Gamma(\Delta_{\uparrow\downarrow 0})$. It is noted that unlike the driving-field free case where only phonons with energy $g\mu_B B_0$ contribute to the spin relaxation, due to the sideband effect caused by the driving field, from Eq. (26) one can see that phonons with energies $\Delta_{\uparrow\downarrow k} = g\mu_B B_0 + k\hbar\Omega$ ($k \neq 0$) also contribute to the spin relaxation. The spin relaxation rate is $T_1^{-1} = 2\Lambda_{\uparrow\uparrow\uparrow\uparrow}$. Particularly, at zero driving field, $T_1^{-1} = 2\Gamma(g\mu_B B_0)$. The spin relaxation time as a function of the THz magnetic field

B_1 and the static magnetic field B_0 , $T_1(B_1, B_0)$, reads

$$\begin{aligned} T_1(B_1, B_0) &\approx T_1(0, B_0) / \left\{ J_0^2(g\mu_B B_1/\hbar\Omega) \right. \\ &\quad \left. + \left(\sum_{k=-\infty}^{-1} + \sum_{k=1}^{\infty} \right) J_k^2\left(\frac{g\mu_B B_1}{\hbar\Omega}\right) \frac{T_1(0, B_0)}{T_0(g\mu_B B_0 + k\hbar\Omega)} \right\} \end{aligned} \quad (28)$$

in which $T_0(g\mu_B B_0 + k\hbar\Omega)$ is the spin relaxation time at same external condition (QD geometry, static magnetic field, temperature, *etc.*) but at different energy $g\mu_B B_0 + k\hbar\Omega$. We approximately take $T_0(g\mu_B B_0 + k\hbar\Omega)$ as the spin relaxation time $T_1(0, B_0^*)$, where B_0^* is determined by the condition that the corresponding Zeeman splitting for the lowest two states is $g\mu_B B_0 + k\hbar\Omega$. This approximation is reasonable when $g\mu_B B_0 + k\hbar\Omega$ is much smaller than the energy difference between the first and second subbands, since the difference in the spin mixing for the lowest two states between the case with a static magnetic field B_0^* and the case with B_0 is marginal.

We first calculate $T_1(0, B_0)$ as a function of B_0 and plot it in Fig. 1(c) as black dotted curve. Facilitated with this quantity, we further obtain $T_1(B_1, B_0)$ in Eq. (28) as a function of B_1 for $B_0 = 1$ T and $\Omega = 1.3$ THz and plot it as black dotted curve in Fig. 1(a). It is seen that this approximate results agrees with the numerical result qualitatively. It is seen from the simplified model that the dominant contribution comes from the term of $J_0^2(\frac{\sigma g\mu_B B_1}{\hbar\Omega})$ in the denominator in Eq. (28) which is zero at $B_1 \approx 2.4$ and 5.6 T, corresponding to the first and the second peaks in Fig. 1(a). In order to reveal which sideband contributes to the peaks, we plot $T_1(B_1, B_0)$ calculated from Eq. (28) with all the sidebands [red solid curve, same as the black dotted curve in Fig. 1(a)], with only the 0, ± 1 -th sidebands (blue dashed curve), and with only the ± 1 , ± 2 -th sidebands (green chain curve) in Fig. 1(c) versus B_1 when $B_0 = 1$ T and $\Omega = 1.3$ THz. It is seen in the figure that the result with only the 0, ± 1 -th sideband agrees with the total approximation result pretty well when $B_1 < 3.5$ T which indicates that the first peak is mainly due to these sidebands. When $B_1 > 3.5$ T, the result including only the ± 1 , and ± 2 -th sidebands is in reasonable agreement with the result with all the sidebands. Therefore the second peak mainly comes from the ± 1 and ± 2 -th sidebands. The oscillations in spin relaxation time are mainly due to oscillations of the sideband amplitude with the strength of the driving field, *i.e.*, the sideband factor $J_k^2(g\mu_B B_1/\hbar\Omega)$ in Eq. (28). The relaxation time $T_0(g\mu_B B_0 + k\hbar\Omega)$ can be larger or smaller than $T_1(0, B_0)$ depending on the details of the SOC mediated spin-phonon coupling,^{29,30,31,32,33,34,35,36} which determines the effect of the THz magnetic field on the spin relaxation time.

At very low temperature, if $g\mu_B B_0 + k\hbar\Omega$ is less than zero, the relaxation process is prohibited because there is no phonon to be absorbed. Therefore, $T_1(0, B_0)/T_0(g\mu_B B_0 + k\hbar\Omega)$ is zero for $g\mu_B B_0 + k\hbar\Omega < 0$. For the case of resonant driven system, only $k \geq 0$ terms remain finite. Among these terms

only the terms with $k = 0$ and 1 are important for small B_1 . $J_0^2(g\mu_B B_1/\hbar\Omega) \approx 1 - 2J_1^2(g\mu_B B_1/\hbar\Omega)$ if $g\mu_B B_1/\hbar\Omega < 1$. Thus the denominator is approximately $1 + J_1^2(g\mu_B B_1/\hbar\Omega)[T_1(0, B_0)/T_0(g\mu_B B_0 + \hbar\Omega) - 2]$. Therefore, $T_0(g\mu_B B_0 + \hbar\Omega)$ becomes an important factor for $T_1(B_1, B_0)$. The three color curves in Fig. 1(a) with $B_0 = 1.0/0.7/0.5$ T, corresponding to $T_1(B_1, B_0)$ being increased/insensitive/decreased with B_1 when $B_1 \leq 1.1$ T. This is because $T_0(g\mu_B B_0 + \hbar\Omega) \approx T_1(0, 2B_0)$ is larger than/approximately/smaller than $T_1(0, B_0)/2$. The same thing happens, if one changes the frequency of the THz magnetic field, as $T_0(g\mu_B B_0 + \hbar\Omega)$ also depends on Ω . The property of the frequency dependence in Fig. 1(b) when $B_1 < 0.7$ T can be understood from the fact that $T_0(g\mu_B B_0 + \hbar\Omega) \approx T_1(0, B_0 + \hbar\Omega/g\mu_B)$ is smaller/a little smaller/larger than $T_1(0, B_0)/2$ when $\Omega = 0.45/0.9/1.8$ THz. This indicates that by properly tuning the frequency of the THz magnetic field, we can change the effect of the THz magnetic field efficiently. For strong THz magnetic field, the sideband factor $J_k^2(g\mu_B B_1/\hbar\Omega)$ is important only for terms with large k where $T_0(g\mu_B B_0 + k\hbar\Omega) \approx T_1(0, B_0 + k\hbar\Omega/g\mu_B)$ is larger than $T_1(0, B_0)$ for large enough k . Moreover, $J_k^2(g\mu_B B_1/\hbar\Omega)$ also decreases with B_1 . Therefore for strong enough THz magnetic field, the spin relaxation time is always larger than $T_1(0, B_0)$ as indicated by the six colored curves in Figs. 1(a) and (b).

IV. CONCLUSIONS

In conclusion, we apply the Floquet-Markov theory to the spin kinetics in 1D InAs QD to study the spin relax-

ation in the presence of the THz driving field. Especially, we study that the spin relaxation under a THz magnetic field which is parallel to a static magnetic field. We find that the spin relaxation time can be effectively manipulated by the driving field depending on its frequency and strength. This offers a new way to control the spin relaxation. The effect is understood as the sideband effect modulates the indirect spin-phonon coupling. The effect of the driving field also depends on the properties of the QD, such as the QD geometry, the strength and symmetries of the spin-orbit coupling, etc., which can be tuned by the gate-voltage, and the static magnetic field. The formulism developed here can be generalized to other systems, such as the two-dimensional electron/hole gas with the SOC to study the spin relaxation. The corresponding kinetic equation can further be used to study the problems such as the AC-field-induced spin polarization and the related spin transport. These are still under investigation and will be published elsewhere.

Acknowledgments

This work was supported by the Natural Science Foundation of China under Grant No. 10574120, the National Basic Research Program of China under Grant No. 2006CNBOL1205, the Natural Science Foundation of Anhui Province under Grant No. 050460203, the Innovation Project of Chinese Academy of Sciences and SRFDP. One of the authors (JHJ) would like to thank J. L. Cheng for helpful discussions.

* Author to whom correspondence should be addressed; Electronic address: mwwu@ustc.edu.cn.

† Mailing Address.

¹ *Semiconductor Spintronics and Quantum Computation*, ed. by D. D. Awschalom, D. Loss, and N. Samarth (Springer-Verlag, Berlin, 2002); I. Žutić, J. Fabian, and S. Das Sarma, Rev. Mod. Phys. **76**, 323 (2004).

² S. A. Wolf, D. D. Awschalom, R. A. Buhrman, J. M. Daughton, S. von Molnár, M. L. Roukes, A. Y. Chtchelkanova, and D. M. Treger, Science **294**, 1488 (2001).

³ Y. Kato, R. C. Myers, D. C. Driscoll, A. C. Gossard, J. Levy, and D. D. Awschalom, Science **299** 1201 (2003).

⁴ E. I. Rashba and A. L. Efros, Phys. Rev. Lett. **91**, 126405 (2003).

⁵ J. L. Cheng and M. W. Wu, Appl. Phys. Lett. **86**, 032107 (2005).

⁶ J. H. Jiang, M. Q. Weng, and M. W. Wu, J. Appl. Phys. **100**, 063709 (2006).

⁷ Y. Tokura, W. G. van der Wiel, T. Obata, and S. Tarucha, Phys. Rev. Lett. **96**, 047202 (2006).

⁸ V. N. Golovach, M. Borhani, and D. Loss, eprint: cond-mat/0601674.

⁹ J. A. Gupta, R. Knobel, N. Samarth, and D. D.

Awschalom, Science **292**, 2458 (2001).

¹⁰ M. Duckheim and D. Loss, Nature Phys. **2**, 195 (2006).

¹¹ F. H. L. Koppens, C. Buizert, K. J. Tielrooij, I. T. Vink, K. C. Nowack, T. Meunier, L. P. Kouwenhoven, and L. M. K. Vandersypen, Nature **442**, 766 (2006).

¹² Y. A. Bychkov and E. Rashba, Sov. Phys. JETP Lett. **39**, 78 (1984).

¹³ G. Dresselhaus, Phys. Rev. **100**, 580 (1955).

¹⁴ M. Grifoni and P. Hänggi, Phys. Rep. **304**, 229 (1998).

¹⁵ S. Kohler, J. Lehmann, and P. Hänggi, Phys. Rep. **406**, 379 (2005).

¹⁶ S. Kohler, T. Dittrich, and P. Hänggi, Phys. Rev. E **55**, 300 (1997).

¹⁷ B. J. Ohlsson, M. T. Björk, M. H. Magnusson, K. Deppert, L. Samuelson, and L. R. Wallenberg, Appl. Phys. Lett. **79**, 3335 (2001); M. T. Björk, B. J. Ohlsson, T. Sass, A. I. Persson, C. Thelander, M. H. Magnusson, K. Deppert, L. R. Wallenberg, and L. Samuelson, Nano Lett. **2**, 87 (2002); M. T. Björk, C. Thelander, A. E. Hansen, L. E. Jensen, M. W. Larsson, L. R. Wallenberg, and L. Samuelson, Nano Lett. **4**, 1621 (2004); Y. Wu, R. Fan, and P. Yang, Nano Lett. **2**, 83 (2002); I. Shorubalko, A. Pfund, R. Leturcq, M. T. Borgström, F. Gramm, E. Müller, E. Gini, and K.

- Ensslin, eprint: cond-mat/0609462.
- ¹⁸ C. L. Romano, S. E. Ulloa, and P. I. Tamborenea, Phys. Rev. B **71** 035336 (2005); P. I. Tamborenea and H. Metiu, Phys. Rev. Lett. **83**, 3912 (1999); Europhys. Lett. **53**, 776 (2001).
 - ¹⁹ G. Ramian, Nucl. Instrum. Methods Phys. Res. Sect. A **318**, 225 (1992).
 - ²⁰ R. Winkler, *Spin-Orbit Coupling Effects in Two-Dimensional Electron and Hole Systems* (Springer, Berlin, 2003).
 - ²¹ D. Grundler, Phys. Rev. Lett. **26**, 6074 (2000).
 - ²² J. H. Shirley, Phys. Rev. **138**, B979 (1965).
 - ²³ T. H. Oosterkamp, L. P. Kouwenhoven, A. E. A. Koolen, N. C. van der Vaart, and C. J. P. M. Harmans, Phys. Rev. Lett. **78**, 1536 (1997).
 - ²⁴ K. B. Nordstrom, K. Johnsen, S. J. Allen, A. -P. Jauho, B. Birnir, J. Kono, and T. Noda, Phys. Rev. Lett. **81**, 457 (1998).
 - ²⁵ J. M. Kikkawa, I. P. Smorchkova, N. Samarth, and D. D. Awschalom, Science **277**, 1284 (1997); J. M. Kikkawa and D. D. Awschalom, Phys. Rev. Lett. **80**, 4313 (1998); J. M. Elzerman, R. Hanson, L. H. Willems van Beveren, B. Witkamp, L. M. K. Vandersypen, and L. P. Kouwenhoven, Nature **430**, 431 (2004); S. Amasha, K. MacLean, Iuliana Radu, D. M. Zumbuhl, M. A. Kastner, M. P. Hanson, and A. C. Gossard, eprint: cond-mat/0607110.
 - ²⁶ M. Q. Weng, M. W. Wu, and L. Jiang, Phys. Rev. B **69**, 245320 (2004).
 - ²⁷ *Semiconductors*, Landolt-Börnstein, New Series, Vol. 17a, ed. by O. Madelung (Springer-Verlag, Berlin, 1987).
 - ²⁸ K. M. Fonseca-Romero, S. Kohler, and P. Hänggi, Chem. Phys. **296**, 307 (2004).
 - ²⁹ H. Westfahl, Jr., A. O. Caldeira, G. Medeiros-Ribeiro, and M. Cerro, Phys. Rev. B **70**, 195320 (2004).
 - ³⁰ J. L. Cheng, M. W. Wu, and C. Lü, Phys. Rev. B **69**, 115318 (2004).
 - ³¹ I. L. Aleiner and V. I. Fal'ko, Phys. Rev. Lett. **87**, 256801 (2001).
 - ³² A. V. Khaetskii and Y. V. Nazarov, Phys. Rev. B **61**, 12639 (2000); *ibid.* **64**, 125316 (2001); C. Lü, J. L. Cheng, and M. W. Wu, Phys. Rev. B **71**, 075308 (2005); C. F. Destefani and S. E. Ulloa, Phys. Rev. B **72**, 115326 (2005); P. San-Jose, G. Zarand, A. Shnirman, and G. Schön, Phys. Rev. Lett. **97**, 076803 (2006).
 - ³³ R. de Sousa and S. Das Sarma, Phys. Rev. B **68**, 155330 (2003).
 - ³⁴ V. N. Golovach, A. Khaetskii, and D. Loss, Phys. Rev. Lett. **93**, 016601 (2004).
 - ³⁵ Y. Y. Wang and M. W. Wu, Phys. Rev. B **74**, 165312 (2006).
 - ³⁶ P. Stano and J. Fabian, Phys. Rev. Lett. **96**, 186602 (2006).
 - ³⁷ V. I. Fal'ko, B. L. Altshuler, and O. Tsyplatyev, Phys. Rev. Lett. **95**, 076603 (2005).